Third International Symposium on the Effects of Surface Geology on Seismic Motion
Grenoble, France, 30 August - 1 September 2006
Paper Number: xxx

Validation and Comparison of One-Dimensional Ground Motion Methodologies

Bob Darragh, Walt Silva, and Nick Gregor
Pacific Engineering and Analysis, El Cerrito, California, United States of America (USA)

ABSTRACT - Both point- and finite-source stochastic one-dimensional ground motion models, coupled to vertically propagating equivalent-linear shear-wave site response models are validated using an extensive set of strong motion data as part of the Yucca Mountain Project. The validation and comparison exercises are presented entirely in terms of 5% damped pseudo absolute response spectra.

The study consists of a quantitative analyses involving modeling nineteen well-recorded earthquakes, **M** 5.6 to 7.4 at over 600 sites. The sites range in distance from about 1 to about 200 km in the western US (460 km for central-eastern US). In general, this validation demonstrates that the stochastic point- and finite-source models produce accurate predictions of strong ground motions over the range of 0 to 100 km and for magnitudes **M** 5.0 to 7.4. The stochastic finite-source model appears to be broadband, producing near zero bias from about 0.3 Hz (low frequency limit of the analyses) to the high frequency limit of the data (100 and 25 Hz for response and Fourier amplitude spectra, respectively).

One dimensional site response method

For these analyses the conventional one-dimensional (1D) approach to estimating the effects of site-specific site conditions on strong ground motions that assumes vertically propagating plane shear-waves for the horizontal components is used. The computational scheme that computes the site response incorporates random vibration theory (RVT) where the control motion power spectrum is propagated through the 1D soil profile using the plane-wave propagators of Silva (1976).

In order to treat possible material nonlinearities, an RVT based equivalent-linear formulation is employed. Random process theory is used to predict peak time domain values of shear-strain based upon the shear-strain power spectrum. The purely frequency domain approach obviates a time domain control motion and, eliminates the need for a suite of analyses based on different input motions. This arises because each time domain analysis may be viewed as one realization of a random process. In the case of the frequency domain approach, the estimates of peak shear-strain as well as oscillator response are, as a result of the random process theory, fundamentally probabilistic in nature. For fixed material properties, stable estimates of site response can then be obtained with a single run.

The major issues involved in the prediction of the effects of site response to strong ground motions include a suitable wave propagation model, the *in situ* strain dependencies of dynamic material properties, and how the effects of material nonlinearities are treated computationally. All three aspects were treated in EPRI (1993) and BSC (2004) by comparing observed strong ground motions to motions predicted by

equivalent-linear and nonlinear approaches using recorded motions from 0.05 to 0.50g (up to 2% shear strains) at four carefully characterized reference sites. Reasonably comprehensive geotechnical models based in part on laboratory testing were developed for Gilroy #2, and Treasure Island in California, Lotung (LSST) in Taiwan and Port Island in Kobe, Japan. The sites possess all of the features that are thought necessary to provide a good validation: recordings of both high- and low-strain ground motions, a dipping interface at least at one site (Gilroy #2), a wide range in material properties from stiff sands and gravel to very soft silts and stiff clays, and deep and shallow surface water tables. The general conclusion resulting from these analyses is that conventional 1D site response analyses incorporating equivalent linear and nonlinear soil behavior based upon careful laboratory testing and with reasonably accurate soil profiles can accurately predict the effect of soils on strong ground motions. Additionally, for response spectral ordinates, both equivalent-linear and fully nonlinear analyses performed equally well in predicting recorded motions over the period range of about 2 to 3 sec to 0.01 sec (peak acceleration). In time domain comparisons, fully nonlinear analyses were superior to equivalent-linear analyses, more closely matching the low amplitude high frequency recordings.

In the validation study, site effects are modeled as vertically propagating shear-waves from the source region (typically at depths near 8 km) to the surface using generic soft rock and deep firm soil generic profiles (Silva et al., 1997). Equivalent-linear analyses are used for shear-wave velocities below about 914 m/sec (near surface at soft rock sites) or depths less than 150 m (deep firm soil sites).

Validation study

The 1D site response analyses involve modeling 19 earthquakes at nearly 600 sites (Table I) using both the stochastic point- and finite-source simulations. The modeling variability is estimated as a chi-square on the average horizontal component response spectra (5% damping) over all earthquakes and sites. Model bias is estimated as the average response spectral misfit over all sites and earthquakes.

The point-source modeling includes initial inversions of Fourier amplitude spectra for stress drop, crustal damping (Q(f)), and site kappa values followed by forward modeling of response spectra. In the finite-source modeling, available slip models are used along with the Q(f) models derived from the point-source inversions.

Stochastic point-source simulation

The conventional stochastic ground motion model uses an ω^2 source model (Brune, 1970, 1971) with a single corner frequency and a constant stress drop (Boore, 1983; Atkinson, 1984). Random vibration theory is used to relate RMS (root-mean-square) values to peak values of acceleration (Boore, 1983), and oscillator response (Boore and Joyner, 1984; Toro, 1985; Silva and Lee, 1987) computed from the power spectra to expected peak time domain values.

Source scaling is provided by specifying two independent parameters, the seismic moment (M_0) and the high-frequency stress parameter or stress drop ($\Delta\sigma$) since it directly scales the Fourier amplitude spectrum for frequencies above the corner frequency (Silva, 1991; Silva and Darragh 1995). The spectral shape of the single-corner-frequency ω^2 source model is then described by the two free parameters M_0 and $\Delta\sigma$. The corner frequency increases with the shear-wave velocity and with increasing stress drop, both of which may be region dependent. Geometrical attenuation is modeled simply as 1/R going

to $1/\sqrt{R}$ (R: hypocentral distance) for distances exceeding two crustal thicknesses with duration as $1/f_c$ plus 0.05 R Herrmann (1985).

The model also includes a high-frequency filter as an attempt to model the observation that acceleration spectral density appears to fall off rapidly beyond some region-dependent maximum frequency. This observed phenomenon truncates the high frequency portion of the spectrum and is responsible for the band-limited nature of the stochastic model. The band limits are the source corner frequency at low frequency and the high frequency spectral attenuation. This spectral fall-off at high frequency has been attributed to near-site attenuation (Hanks, 1982; Anderson and Hough, 1984) or to source processes (Papageorgiou and Aki, 1983) or perhaps to both effects. The attenuation directly below the site in modeled by kappa (Anderson and Hough, 1984) while the crustal path attenuation from the source to just below the site is modeled with the region and frequency- dependent quality factor Q(f) (Table II). Kappa has been found to depend on surficial geology at rock sites becoming smaller as rock quality improves or with increasing stiffness (Silva and Darragh, 1995), supporting the high frequency spectral fall-off dependence on site effects. Based on the inversions, rock and soil site total kappa (shallow geotechnical plus shallow crust) values are set at 0.04 sec at low strains at all sites for both point- and finite-source validations.

Factors that effect strong ground motions such as surface topography, finite and propagating seismic sources, laterally varying near-surface velocity and Q gradients, and random inhomogeneities along the propagation path are not included in the model. While some or all of these factors are generally present in any observation of ground motion and may exert controlling influences in some cases, the simple and elegant stochastic point-source model appears to be robust in predicting median or average properties of ground motion for engineering characterization (Boore 1983; McGuire et al., 1984; Silva et al., 1988; Schneider et al., 1993; BSC, 2004).

An example of the point-source validation showing both variability and bias estimates, based on modeling recorded motions (5% damped spectra), for sixteen earthquakes (503 sites and distances to about 450 km) is shown in Figure 1. The bias and variability estimates (with each earthquake having equal weight) show near zero bias for frequencies from 1 Hz and above. The stochastic point-source model shows a stable and significant negative bias (over-prediction) from about 1 to 0.3 Hz (the approximate lower frequency limit of the analyses). This low frequency ($\leq$ 1 Hz) overprediction (bias) at large magnitude is considered a model shortcoming (Silva et al., 1997) and led Atkinson and Silva (1997) to consider a 2-corner model for tectonically active regions. For an engineering model, this error is not considered serious as it reflects an overprediction and predictions may be adjusted or simply reflect conservative design motions. The variability estimates are generally uniform at about 0.5 to 0.6 (natural log units) at 1 Hz and above increasing with decreasing frequency. The increase in variability at low frequency is similar to that seem in empirical relations (Abrahamson and Shedlock, 1997) and reflects site-to-site variability not captured by the model, such as depth to basement material.

Stochastic finite-fault simulation

In the near-source region of large earthquakes, aspects of a finite-source including rupture propagation, directivity, and source-receiver geometry can be significant and may be incorporated into strong ground motion predictions. To accommodate these effects, a methodology that combines the aspects of finite-earthquake-source modeling techniques (Hartzell, 1978; Irikura 1983) with the stochastic point-source ground motion model (Boore, 1983) has been developed to produce response spectra as well as time histories appropriate for engineering design (Silva et al., 1990; Schneider et al., 1993; Silva et al.,

1997; Beresnev and Atkinson, 1997). In this case however, the stochastic point-source is substituted for the empirical Green function and peak amplitudes; PGA, PGV, and response spectra are estimated using random process theory.

Modeling of the Landers (Wald and Heaton, 1994a), Kobe (Wald, 1996) and Northridge (Hartzell et al. 1996) earthquakes suggests that a mixture of both constant rise time and constant slip velocity may be present. Longer rise times seem to be associated with areas of larger slip with the ratio of slip-to-rise time (slip velocity) being depth dependent. Lower slip velocities (longer rise times) are associated with shallow slip resulting in relatively less short period seismic radiation. This result may explain the general observation that shallow slip is largely aseismic. The significant contributions to strong ground motions appear to originate at depths exceeding about 4 km (Campbell, 1993; Boore et al., 1994) as the fictitious depth term in the empirical attenuation relationships suggests. Finite-fault models generally predict unrealistically large strong ground motions for large shallow (near surface) slip using rise times or slip velocities associated with deeper (> 4 km) zones of slip.

Finite source parameters include a constant slip velocity (to reduce the observed dependence of motions on static stress drop) of 100 cm/sec and subevent stress-drop of 60 bars. Based on initial validations of the approach (Silva et al. 1997), the subevent stress drop was reduced to 10 bars to accommodate the observed reduction in short-period motions for shallow-slip dominated earthquakes. For shallow slip dominated earthquakes, more than 20% of the moment released over the top 5 km of the crust, short period ($\leq$ 1 to 2 sec) motions appeared to be lower by about 50 to 100% compared to deep slip dominated earthquakes of the same **M**. This observation suggested fundamentally different source dynamics for shallow slip earthquakes necessitating a dramatic reduction of the subevent stress drop over the entire rupture surface (Silva et al., 1997). This observed reduction in short period motions is also reflected in point-source stress drops when separating deep and shallow slip earthquakes. Taking all events the median stress drop is about 50 bars (Table III) with a variability of 0.5 (σ_{ln}). Separating deep and shallow slip dominated earthquakes, the corresponding stress drops are about 57 bars and 31 bars with reduced associated variabilities of about 0.4 (σ_{ln}) each. This is an example of epistemic variability masquerading as aleatory variability (actually two populations), and where increased knowledge has allowed a discrimination, resulting in a lowering of the aleatory variability reflecting within population dispersion. Vertically propagating shear-waves combined with kappa (Anderson and Hough, 1984) are assumed for amplification while geometrical attenuation from each subfault to the site is modeled via the method of Ou and Herrmann (1990), along with a Q(f) term for crustal damping. To introduce heterogeneity of the earthquake source process into the stochastic finite-fault model, the location of the sub-events within each subfault (Hartzell, 1978) are randomized as well as the subevent rise time. The rectangular fault is discretized to provide the locations of the sub-events all with **M** 5.

This simple method is fundamentally broadband and an example of the validation exercise showing both variability and bias estimates, based on modeling recorded motions (5% damped spectra), for eighteen earthquakes (about 600 sites) are shown in Figure 2. The broadband model is largely unbiased and captures site-to-site variations acceptably well, over a wide frequency range.

Conclusions

Model bias and variabilities were estimated for 16 of these earthquakes at over 503 sites for the point-source model and 594 sites (18 earthquakes) for the finite-source

model (BSC, 2004). In general, the bias estimates were low and the variabilities small (Figures 1 and 2). For the point-source model, the final bias and variability estimates computed for all of these sites and earthquakes showed near zero bias for frequencies from 1 Hz and above. The model shows a stable and significant negative bias (overprediction) from about 1 to 0.3 Hz (the approximate lower frequency limit of the analyses). The variability estimates are generally uniform at about 0.5 to 0.6 (natural log units) at 1 Hz and above. For the finite-source model the low-frequency bias is significantly reduced and model variability is about 0.7 (natural log units) at 1 Hz and above. The larger variability over the point-source results (Figure 1) is likely due to the additional earthquakes (Kobe, Kocaeli and Duzce). These variability estimates are considered low as the majority of the data are for **M** < 6.5 and the site range in distances extends out to about 200 km in the western US (460 km for Saguenay).

The combined RVT point/finite-source/RVT equivalent-linear site-response modeling using vertically propagating S-waves appears to capture the significant and stable features of crustal amplification and site response reflected in strong motion recordings at both soft-rock and deep soil sites for soil column thickness of up to about 300 m.

For earthquakes dominated by shallow slip (at least 20% of the total moment released over the top 5 km) the subevent stress drop had to be reduced from 60 bars (nominal value) to 10 bars for the finite-source models, resulting in significantly lower short-period motions than expected. For the point source model, the average stress drop was about 50 bars (σ_{ln} near 0.5) averaged over all earthquakes. Separating shallow and deep slip dominated earthquakes results in a stress drop of about 30 and 60 bars, respectively, with a corresponding reduction in σ_{ln} to about 0.4. Epistemic uncertainty had been previously mapped into aleatory variability, before the dependence of point-source stress drop on slip depth was resolved.

References

Abrahamson, N.A and K.M. Shedlock (1997). Overview. *Seismological Research Letters*, 68(1), 9-23.

Anderson, J. G. and S. E. Hough (1984). A model for the shape of the Fourier amplitude spectrum of acceleration at high frequencies. *Bulletin of the Seismological Society of America,* 74(5), 1969-1993.

Atkinson, G.M. and W. Silva (1997). An empirical study of earthquake source spectra for California earthquakes. *Bulletin of the Seismological Society of America*, 87(1), 97-113.

Atkinson, G.M. (1984). Attenuation of strong ground motion in Canada from a random vibrations approach. *Bulletin of the Seismological Society of America*, 74(5), 2629-2653.

Beresnev, I. A. and G. M. Atkinson (1997). Modeling finite-fault radiation from the ω^n spectrum. *Bulletin of the Seismological Society of America*, 87(1), 67-84.

Boore, D.M. (1983). Stochastic simulation of high-frequency ground motions based on seismological models of the radiated spectra. *Bulletin of the Seismological Society of America*, 73(6), 1865-1894.

Boore, D.M. and W. B. Joyner (1984). A note on the use of random vibration theory to predict peak amplitudes of transient signals. *Bulletin of the Seismological Society of America*, 74, 2035-2039.

Boore, D.M., W.B. Joyner, and T.E. Fumal (1994). Estimation of response spectra and peak accelerations from western North American earthquakes: and interim report. Part 2. U.S. Geological Survey Open-File Report. 94-127.

Brune, J.N. (1970, 1971). Tectonic stress and the spectra of seismic shear waves from earthquakes. *Journal of Geophysical Research* 75, 4997-5009, 76, 5002.

BSC (Bechtel SAIC Company) (2004). Development of earthquake ground motion input for preclosure seismic design and postclosure performance assessment of a geologic repository at Yucca Mountain, NV, MDL-MGR-GS-000003 REV 1. Las Vegas, Nevada: Bechtel SAIC Company.

Campbell, K.W. (1993) Empirical prediction of near-source ground motion from large earthquakes. in V.K. Gaur, ed., *Proceedings, International Workshop on Earthquake Hazard and Large Dams in the Himalaya.* INTACH, New Delhi, p. 93-103.

Electric Power Research Institute (1993). Guidelines for determining design basis ground motions. Palo Alto, California: Electric Power Research Institute, vol. 1-5, EPRI TR-102293.

Graves, R.W. (1994). Simulating the 3D basin response in The Portland and Puget Sound Regions from large subduction zone earthquakes. USGS Award: 1434-93-G-2327, Annual Technical Report.

Hanks, T.C. (1982). f_{max}. *Bulletin of the Seismological Society of America,* 72, 1867-1879.

Hartzell, S.H. (1978). "Earthquake aftershocks as Green's functions." *Geophysical Research Letters*, 5, 1-4.

Hartzell, S.H. (1989). Comparison of seismic waveform inversion results for the rupture history of a finite fault: application to the 1986 North Palm Springs, California, earthquake. *Journal of Geophysical Research*, 94(B6), 7515-7534.

Hartzell, S.H. and T.H. Heaton (1983). Inversion of strong ground motion and teleseismic waveform data for the fault rupture history of the 1979 Imperial Valley, California, earthquake. *Bulletin of the Seismological Society of America*, 73(6), 1553-1583.

Hartzell, S.H., and T. H. Heaton (1986). Rupture history of the 1984 Morgan Hill, California, earthquake from the inversion of strong motion records. Bulletin *of the Seismological Society of America*, 76(3), 649-674.

Hartzell, S.H. and M. Iida (1990). Source complexity of the 1987 Whittier Narrows, California, earthquake from the inversion of strong motion records. *Journal of Geophysical Research,* 95(B8), 12475-12485.

Hartzell, S., C. Langer and C. Mendoza (1991). Application of an iterative least-squares waveform inversion of strong-motion and teleseismic records to the 1978 Tabas, Iran. *Bulletin of the Seismological Society of America*, 81(2), 305-331.

Hartzell, S., C. Langer and C. Mendoza (1994). Rupture histories of eastern North American earthquakes. *Bulletin of the Seismological Society of America*, 84(6), 1703-1724.

Hartzell, S., P. Liu and C. Mendoza (1996). "The 1994 Northridge, California, earthquake: Investigation of rupture velocity, rise time, and high-frequency radiation." *Journal of Geophysical Research,* 101(B9), 20,091-20,108.

Heaton, T. H. (1982). The 1971 San Fernando earthquake: A double event? *Bulletin of the Seismological Society of America,* 72, 2037-2062.

Herrmann, R. B. (1985). An extension of random vibration theory estimates of strong ground motion to large distance. . *Bulletin of the Seismological Society of America*, 75, 1447-1453.

Irikura, K. (1983). Semi-empirical estimation of strong ground motions during large earthquakes. *Bulletin of the Disaster Prevention Research Institute*, Kyoto Univ., 33, 63-104.

Liu, H-L, and D. V. Helmberger (1983). The near-source ground motion of the 6 August 1979 Coyote Lake, California, earthquake. *Bulletin of the Seismological Society of America*, 73(1), 201-218.

McGuire, R. K., A. M. Becker and N. C. Donovan (1984). Spectral estimates of seismic shear waves. . *Bulletin of the Seismological Society of America*, 74(4), 1427-1440.

Ou, G.B. and R. B. Herrmann (1990). Estimation theory for strong ground motion. *Seismological Research Letters*. 61.

Papageorgiou, A.S., and K. Aki (1983). A specific barrier model for the quantitative description of inhomogeneous faulting and the prediction of strong ground motion, part I, Description of the model. *Bulletin of the Seismological Society of America*, 73(4), 693-722.

PEARL (2002). Validation of 1-D numerical simulation procedures. 35 pp.

Schneider, J.F., W.J. Silva, and C.L. Stark (1993). Ground motion model for the 1989 **M** 6.9 Loma Prieta earthquake including effects of source, path and site. *Earthquake Spectra,* 9(2), 251-287.

Silva, W.J. (1976). Body waves in a layered anelastic solid. *Bulletin of the Seismological Society of America*, 66(5), 1539-1554.

Silva, W.J. (1991). Global characteristics and site geometry. Chapter 6 in *Proceedings: NSF/EPRI Workshop on Dynamic Soil Properties and Site Characterization.* Palo Alto, California: Electric Power Research Institute, NP-7337.

Silva, W.J., N. Abrahamson, G. Toro and C. Costantino (1997). Description and validation of the stochastic ground motion model. Report Submitted to Brookhaven National Laboratory, Associated Universities, Inc. Upton, New York 11973, Contract No. 770573.

Silva, W.J., and R. Darragh (1995). Engineering characterization of earthquake strong ground motion recorded at rock sites. Palo Alto, California, Electric Power Research Institute, TR-102261.

Silva, W. J., R. Darragh, C. Stark, I. Wong, J. C. Stepp, J. Schneider, and S-J. Chiou (1990). A methodology to estimate design response spectra in the near-source region of large earthquakes using the band limited-white-noise ground motion model". *Proceedings of the Fourth U.S. Conference on Earthquake Engineering,* Palm Springs, California. 1, 487-494.

Silva, W.J. and K. Lee (1987). *WES RASCAL code for synthesizing earthquake ground motions.* State-of-the-Art for Assessing Earthquake Hazards in the United States, Report 24, U.S. Army Engineers Waterways Experiment Station, Miscellaneous Paper S-73-1.

Silva, W. J., T. Turcotte, and Y. Moriwaki, (1988). Soil response to earthquake ground motion, Electric Power Research Institute, Walnut Creek, California, Report No. NP-5747.

Toro, G. R. (1985). Stochastic model estimates of strong ground motion. In *Seismic Hazard Methodology for Nuclear Facilities in the Eastern United States*, Appendix B, R. K. McGuire, ed., Electric Power Research

Institute, Project P101-29.
Wald, D.J. (1996). Slip history of the 1995 Kobe, Japan, earthquake determined from strong motion, teleseismic and geodetic data. *Journal of Physics of the Earth*, 44, 489-503.
Wald, D.J., T. H. Heaton (1994a). Spatial and temporal distribution of slip for the 1992 Landers, California, earthquake. *Bulletin of the Seismological Society of America*, 84(3), 668-691.
Wald, D.J., T. H. Heaton (1994b). A dislocation model of the 1994 Northridge, California, earthquake determined from strong ground motions. U.S. Geological Survey, Open-File Rpt. 94-278.
Wald, D.J., D.V. Helmberger, and T.H. Heaton (1991). Rupture model of the 1989 Loma Prieta earthquake from the inversion of strong motion and broadband teleseismic data. *Bulletin of the Seismological Society of America*, 81(5), 1540-1572.
Wald, D.J., D.V. Helmberger and S.H. Hartzell (1990). Rupture process of the 1987 Superstition Hills earthquake from the inversion of strong-motion data. Bulletin of the Seismological Society of America, 80(5), 1079-1098.

Table I. Earthquake Information

Earthquake Name	Year	**M**	M_0 x 10^{25} (dyne-cm)	Fault Distances (km)	Rock Sites	Soil Sites	Total Sites
San Fernando, CA	1971	6.6	8.91	3 – 218	21	18	39
Tabas, Iran	1978	7.4	141.0	3 – 90	3	1	4
Coyote Lake, CA	1979	5.7	0.40	3 – 30	3	7	10
Imperial Valley, CA	1979	6.4	4.47	1 – 50	2	33	35
Imperial Valley (AS)	1979	5.3	0.10	12 – 52	0	16	16
Morgan Hill, CA	1984	6.2	2.24	1 – 70	8	21	29
Nahanni, Canada	1985	6.8	17.8	6 – 16	3	0	3
N. Palm Springs, CA	1986	6.0	1.12	1 – 90	9	20	29
Whittier Narrows, CA	1987	6.0	1.12	10 – 80	18	70	88
Superstition Hills(B), CA	1987	6.4* (6.7)	4.47	1 – 28	1	10	11
Saguenay, Canada	1988	5.8	0.56	47 – 460	22	0	22
Loma Prieta, CA	1989	6.9	25.1	5 – 90	33	20	53
Little Skull Mtn., NV**	1992	5.7,4.4,4.2	0.40	15 – 98	8	0	8
Landers, CA	1992	7.2	70.8	1 – 177	5	52	57
Cape Mendocino, CA	1992	6.8	17.8	8 – 45	1	4	5
Northridge, CA	1994	6.7	12.6	7 – 147	44	78	122
Kobe, Japan	1995	6.9	25.1	1 – 158	6	19	25
Kocaeli, Turkey	1999	7.4	141.0	1 – 472	10	22	32
Duzce, Turkey	1999	7.1	50.1	1 – 189	13	9	22
Total					210	400	610

* Preferred **M** ** **M** for mainshock, then **M** for two aftershocks

Table II. Earthquake Model Parameters

Earthquake	Stress Drop Inversion (bars)	Number of Sites	Avg. Rise Time (sec)	$Q_0(f)^{\eta}$	Slip Model Reference
San Fernando, CA*	36.1	39	0.80	$264f^{0.6}$	Modified Heaton (1982)
Tabas, Iran*	21.5	4	1.44	$289f^{0.6}$	Hartzell et al. (1991)
Coyote Lake, CA	70.1	10	0.17	$176f^{0.6}$	Liu and Helmberger (1983)
Imperial Valley, CA*	23.2	35	0.65	$264f^{0.6}$	Hartzell & Heaton (1983)
Imperial Valley (AS)	28.7	16	---	$264f^{0.6}$	Point source
Morgan Hill, CA*	49.0	29	0.29	$176f^{0.6}$	Hartzell & Heaton (1986)
Nahanni, Canada*	13.4	3	0.57	$317f^{0.86}$	Hartzell et al. (1994)
N. Palm Springs, CA	62.8	29	0.084	$371f^{0.6}$	Hartzell (1989)
Whittier Narrows, CA	95.7	88	0.83	$264f^{0.6}$	Hartzell & Iida (1990)
Superstition (B), CA*	43.4**(26.6)	11	0.60	$264f^{0.6}$	Wald et al. (1990)
Saguenay, Canada	572.2	22	0.049	$317f^{0.86}$	Hartzell et al. (1994)
Loma Prieta, CA	73.7	53	1.04	$176f^{0.6}$	Wald et al. (1991)
Little Skull Mtn., NV	63.7	8	0.26	$256f^{0.47}$	Derived
Landers, CA*	40.7	57	2.17	$371f^{0.6}$	Wald and Heaton (1994a)
Cape Mendocino, CA	27.2	5	0.74	$176f^{0.6}$	Graves (1994)
Northridge, CA	62.9	122	0.99	$264f^{0.6}$	Wald and Heaton (1994b)
Kobe, Japan	---	25	0.66	$184f^{0.6}$	Wald (1996)
Kocaeli, Turkey	---	32	1.67	$180f^{0.6}$	PEARL (2002)
Duzce, Turkey	---	22	1.27	$180f^{0.6}$	PEARL (2002)

* Earthquakes with more than 20% moment released over the top 5 km.

** Preferred stress drop consistent with the preferred magnitude (see Table I)

Table III. Western North America Stress Parameter

Data Set	Stress Drop (bars)	σ_{ln}
All	46.9	0.47
Shallow Slip	30.6	0.37
Deep Slip	56.6	0.38

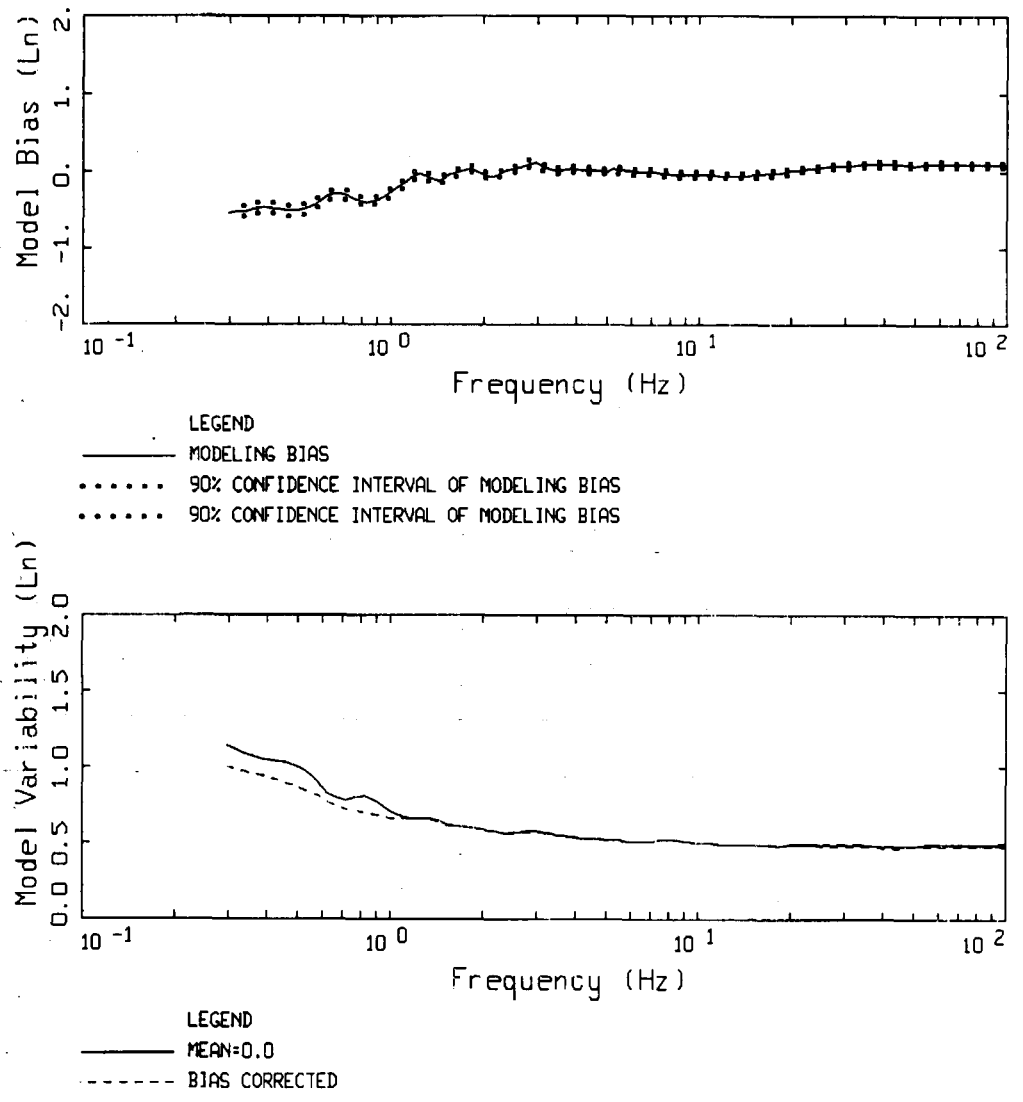

Figure 1: Bias and variability estimates for all earthquakes computed over all 503 sites for the point-source model.

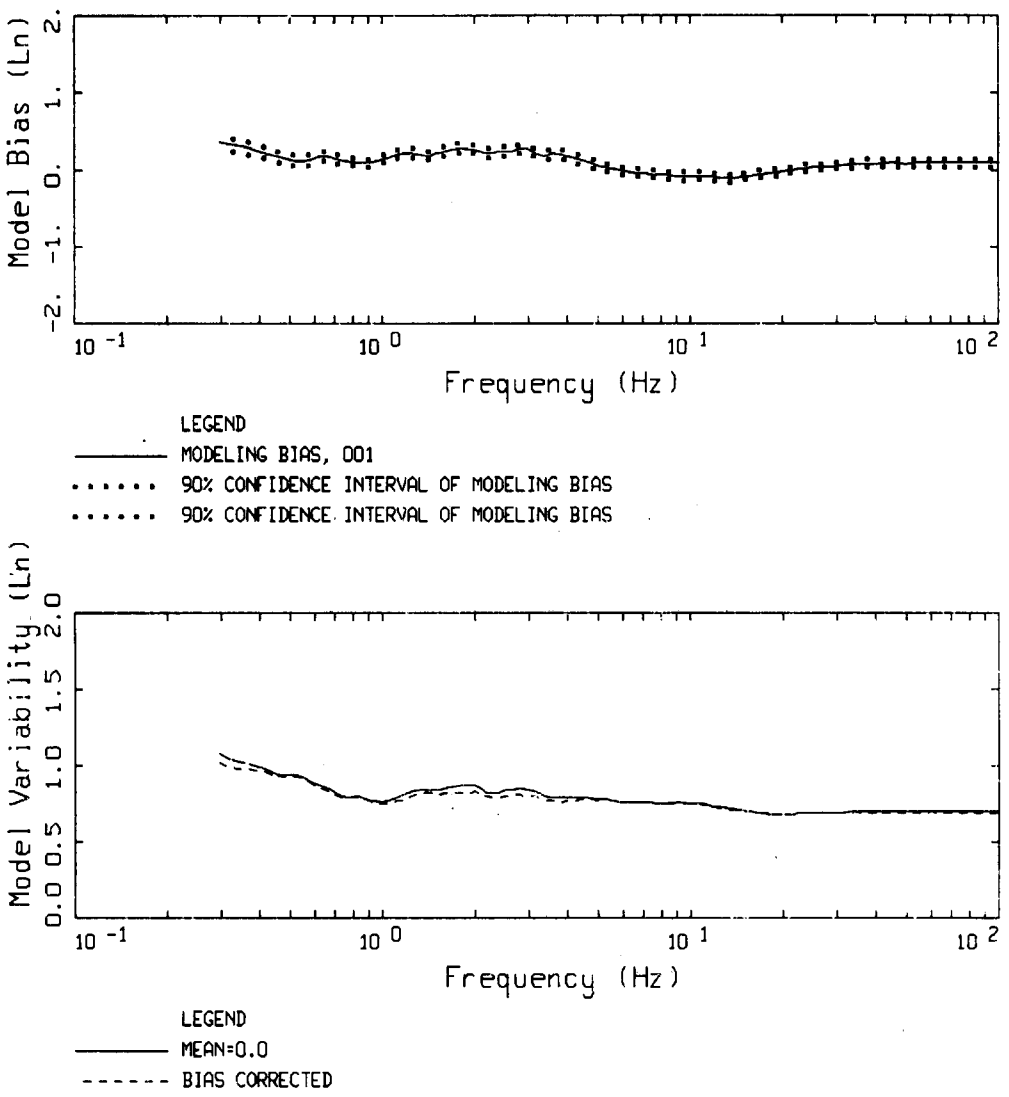

Figure 2: Bias and variability estimates for all earthquakes computed over 594 sites for the finite-source model.